

Utah State University

DigitalCommons@USU

All Graduate Theses and Dissertations

Graduate Studies

12-2008

Intergranular Phases in Cyclically Annealed YBa₂Cu₃O_{7-x} and Their Implications for Critical Current Densities

Andrew Peter Clarke
Utah State University

Follow this and additional works at: <https://digitalcommons.usu.edu/etd>



Part of the [Condensed Matter Physics Commons](#), and the [Materials Science and Engineering Commons](#)

Recommended Citation

Clarke, Andrew Peter, "Intergranular Phases in Cyclically Annealed YBa₂Cu₃O_{7-x} and Their Implications for Critical Current Densities" (2008). *All Graduate Theses and Dissertations*. 88.

<https://digitalcommons.usu.edu/etd/88>

This Thesis is brought to you for free and open access by the Graduate Studies at DigitalCommons@USU. It has been accepted for inclusion in All Graduate Theses and Dissertations by an authorized administrator of DigitalCommons@USU. For more information, please contact digitalcommons@usu.edu.



INTERGRANULAR PHASES IN CYCLICALLY ANNEALED $\text{YBa}_2\text{Cu}_3\text{O}_{7-x}$ AND
THEIR IMPLICATIONS FOR CRITICAL
CURRENT DENSITIES

by

Andrew P. Clarke

A thesis submitted in partial fulfillment
of requirements for the degree

of

MASTER OF SCIENCE

in

Physics

Approved:

Wilford Hansen
Major Professor

Jan J. Sojka
Committee Member

J. R. Dennison
Committee Member

Byron R. Burnham
Dean of Graduate Studies

UTAH STATE UNIVERSITY
Logan, Utah

2008

Copyright © Elsevier Sequoia 1991

All Rights Reserved

ABSTRACT

Intergranular Phases in Cyclically Annealed $\text{YBa}_2\text{Cu}_3\text{O}_{7-x}$
and Their Implications for Critical Current Densities

by

Andrew P. Clarke, Master of Science

Utah State University, 2008

Major Professor: Dr. Wilford N. Hansen
Department: Physics

We report changes in the intergranular material and grain morphology of $\text{YBa}_2\text{Cu}_3\text{O}_{7-x}$ during cyclic anneals between 780 and 980 °C in oxygen at atmospheric pressure. Two endothermic reactions were detected: (a) the eutectic reaction of $\text{YBa}_2\text{Cu}_3\text{O}_{7-x}$ with CuO and BaCuO_2 at 900 °C (enthalpy ΔH_a) and (b) the peritectic reaction of $\text{YBa}_2\text{Cu}_3\text{O}_{7-x}$ with CuO at 950 °C (ΔH_b). During the first anneal, only reaction (b) is detected, and although it should only occur if there is an excess of CuO , its signature is present in all published data. Cyclic annealing causes a monotonic decrease in ΔH_b and an increase in ΔH_a , larger average grain sizes, and greater volume fraction of the superconducting phase. A steady state is reached after 10 cycles at which point $\Delta H_b = 0$. We propose a model that explains the origin of the intergranular CuO and the changes in the intergranular material composition with cyclic annealing.

(45 pages)

ACKNOWLEDGMENTS

This work was supported by the United States Department of Energy, Office of Basic Energy Science, Division of Material Sciences and a grant from the Associated Western Universities, Inc. I would like to express my deep gratitude to Dr. Ricardo B. Schwarz for his guidance, support, and supervision of this work during my time at Los Alamos, and his continued moral support and friendship since. I also thank Joseph D. Thompson for his measurements and interpretations, editing contributions, and many helpful discussions. I am also indebted to Philip Nash, Martin Maley, and Jeff Willis for their many helpful discussions.

The final presentation of this work as a thesis, long after it was finished, was made possible by of the patience and support of my thesis committee: Professors Wilford Hansen, Jan Sojka, and JR Dennison.

I give special thanks to my wife, Leanne, who always supports my dreams and my efforts to make them real.

Andrew P. Clarke

CONTENTS

	Page
ABSTRACT	iii
ACKNOWLEDGMENTS	iv
LIST OF FIGURES	vi
CHAPTER	
I. INTRODUCTION	1
II. PREVIOUS WORK—LITERATURE REVIEW	2
III. EXPERIMENTAL PROCEDURE	5
IV. RESULTS	8
Phase Transformations During the Synthesis of $\text{YBa}_2\text{Cu}_3\text{O}_{7-x}$	8
Chemistry of the Intergranular Material	12
Grain Growth During Cyclic Annealing	15
Changes in the Volume Fraction of Superconducting Phase	19
V. DISCUSSION	21
Presence of CuO at the Surface of $\text{YBa}_2\text{Cu}_3\text{O}_{7-x}$	21
Change in the Intergranular Material Composition with Cyclic Annealing	25
VI. CONCLUSIONS	29
REFERENCES	30
APPENDIX	33
Permissions, Waivers, and Licenses	33

LIST OF FIGURES

Figure	Page
1 X-ray diffraction patterns of mixed oxide powders after mechanical alloying	9
2 DSC trace for the first oxygen anneal of the mixed alloy powders mechanically alloyed for 10	10
3 DSC traces for five consecutive cyclic oxygen anneals	11
4 Area under the DSC peaks D and F vs. number of cyclic oxygen anneals	12
5 Scanning electron micrographs of samples polished after 1 (a) and 14 (b) cyclic oxygen anneals	13
6 X-ray diffraction patterns of $\text{YBa}_2\text{Cu}_3\text{O}_{7-x}$ cyclically annealed once (a) and 20 (b) times	15
7 Scanning electron micrograph of samples cyclically annealed 1 (a), 8 (b) and 67 (c) times	16,17
8 Average size of the $\text{YBa}_2\text{Cu}_3\text{O}_{7-x}$ crystals vs. number of cyclic oxygen anneals	18
9 Magnetic susceptibility of $\text{YBa}_2\text{Cu}_3\text{O}_{7-x}$ vs. number of cyclic oxygen anneals	20
10 Schematic isothermal sections of the ternary $\text{Y}_2\text{O}_3 - \text{CuO} - \text{BaO}$ phase diagram of Aselage and Keefer [32]	27
11 Semi-log plot of the enthalpy of peak D vs. number of cyclic oxygen anneals	28

CHAPTER I

INTRODUCTION

Among the requirements for a useable superconductor are high critical current density, J_c , and high critical magnetic field, H_{c2} . Under both these requirements, polycrystalline compacts of $\text{YBa}_2\text{Cu}_3\text{O}_{7-x}$ have not performed as well as oriented thin films. So far, the best bulk specimens have been highly-textured, large-grained samples prepared by the melt-textured-growth process [1, 2], but even in these samples J_c is only approximately 1% of the J_c in oriented thin films [3]. Several authors [4-8] have compared the measured J_c with that deduced from magnetic hysteresis measurements using the Bean Model [9-12]. These comparisons show that the intergranular J_c in bulk $\text{YBa}_2\text{Cu}_3\text{O}_{7-x}$ is at least as large as that measured in thin films. Theoretical models [13] have been developed to explain the measured transport properties in bulk $\text{YBa}_2\text{Cu}_3\text{O}_{7-x}$ in terms of superconducting grains connected by superconducting “weak links,” and calculations based on these models explain both the low measured critical current density and the further decrease in this current under relatively weak applied magnetic fields.

Although investigators now agree that the relatively low J_c in bulk $\text{YBa}_2\text{Cu}_3\text{O}_{7-x}$ is mainly caused by second-phase intergranular material, our understanding of these phases is still limited. In this paper we study intergranular reactions that take place when annealing these materials in oxygen at temperatures close to 900 °C. We further study the evolution of the intergranular material under cyclic annealing in oxygen between 780 °C and 980 °C.

CHAPTER II

PREVIOUS WORK—LITERATURE REVIEW

The phenomenon of superconductivity was first reported in 1911 by Onnes [14], who detected it in mercury at critical temperature, T_c , equal to 4.12 K. The discovery of other superconductors soon followed, with lead (Pb) at $T_c = 7$ K and niobium nitride (NbN) at 16 K.

The expulsion of static magnetic fields by superconductors was first reported by Meissner and Ochsenfeld [15] in 1933. The Meissner Effect differed from the classical effect described by Lenz's Law, in that Lenz's Law only predicts the expulsion of *changing* magnetic fields due to classical diamagnetism, whereas superconductors expel even *static* magnetic fields. This discovery allowed researchers to discern between true superconducting behavior and simple low resistivity in mixed-phase samples, and in samples through which electrical current could not be easily passed. London and London [16] showed, in 1935, that the Meissner Effect was caused by the minimization of the electromagnetic free energy of the current-carrying superconductor, and was continuous at a surface boundary, with a characteristic penetration into the superconductor called the London Penetration Depth.

In 1957, Abrikosov [17] published a paper proposing the existence of two classes of superconductor, now known as Type I and Type II, based on the Ginsburg-Landau theory of superconductivity [18]. Type I describes materials with discrete transition field strength, H_c , above which superconductivity ceases, and the latter materials (Type II) that exhibit a mixed-phase transition regime bounded by first and second discrete critical field

strengths, H_{c1} and H_{c2} . This gave researchers insight into so-called “spin glass” (Type II) materials that pin quanta of magnetic field (fluxons). This had later significance in understanding the mechanisms involved in high- T_c superconductors.

In 1962, Josephson [19] predicted the tunneling of Cooper pairs, the basic current carriers in the superconducting theory of Bardeen, Cooper, and Schrieffer [20], across thin insulating barriers. The Josephson Effect would later help explain the disparity between the measured critical current density, J_c , at which superconductivity ceases, and the value predicted from measurements of H_c , using the Bean model [9-12], in mixed-phase superconductors. Significantly, the Josephson Effect became the basis for a new ultra-sensitive Superconducting Quantum Interference Device (SQUID) magnetometer that allowed researchers to detect superconducting behavior in small fractions of mixed-phase samples.

In 1986, Bednorz and Muller [21] first reported the onset of superconducting behavior in mixed phase BaLaCuO powders. They analyzed their samples using powder x-ray diffractometry and isolated the superconducting phase Ba:La₂Cu₃O_x, where Ba represented only a few atomic percent. Once isolated as the superconducting phase, exact mixtures were made and single phase samples could be examined. SQUID magnetometer studies indicated a transition to superconductivity at $T_c = 36\text{K}$, roughly twice the critical temperature of any previously reported superconductors.

These *cuprate perovskite* materials were studied further, and in 1987 Wu et al. [22] reported a superconducting phase within the YBaCuO system at YBa₂Cu₃O_{7-x} with a $T_c = 93\text{K}$. This caused much excitement and an explosion of research into these high- T_c superconductors, or HTSC.

Further development of the new HTSC materials would be required if they were to become useable, for though these brittle ceramics expelled magnetic fields as strong Type II superconductors, they could carry very little superconducting current [23-25]. In the research community there were reports [26-28] of thin films of $\text{YBa}_2\text{Cu}_3\text{O}_{7-x}$ that exhibited two orders of magnitude higher critical current densities than the best bulk samples measured, and no one was sure why. With similar H_c values, this difference inferred that the bulk samples consisted of superconducting grains separated by layers of insulating second phase materials, and that current densities were therefore limited by Josephson Effect tunneling across these intergranular “weak links.”

We undertook the research reported here with the goal of determining the compositional and thermodynamic pathways taken by an amorphous powder of Y, Ba, Cu, and oxygen on its way to becoming $\text{YBa}_2\text{Cu}_3\text{O}_{7-x}$ crystalline. In doing this, we hoped to discover the processes that lead to the formation of the intergranular material limiting J_c , and perhaps uncover a remedy to its formation.

CHAPTER III

EXPERIMENTAL PROCEDURE

We mixed BaO₂, CuO, and Y₂O₃ inside an argon-atmosphere glovebox (O₂ and H₂O content less than 1 ppm) to make powder samples with the composition YBa₂Cu₃O_x. The BaO₂ was reagent grade from J. T. Baker Chemical Co. (Phillipsburg, NJ 08865) with an assay of 98 wt.% min. (major impurity BaCO₃ with less than 0.002 wt.% lead and less than 0.03 wt.% iron). The CuO was 99.999 wt.% from Aesar/Johnson-Matthey (Seabrook, NH 03874). The Y₂O₃ was 99.999 wt.% from Research Chemicals (Phoenix, AZ 85063). The CuO and Y₂O₃ powders were baked inside the glovebox for 1 h at 750 °C to remove absorbed water.

We used a high-energy Spex model 8000 mixer located inside the glovebox to mechanically alloy 6 g of powder using a hardened steel vial and hardened steel balls. Mechanical alloying (MA) is a high-energy ball-milling process originally developed to prepare nickel-based precipitation-hardened alloy powders [29]. Recently, researchers have also applied MA to the synthesis of amorphous metallic alloy powders [30]. During MA, the powder particles trapped between colliding balls are repeatedly fractured and cold-welded. This refines the powder structure, and for sufficiently long MA time, it leads to the formation of a true alloy. With MA there is always the danger that the milling may erode the vial and/or the balls and introduce impurities into the powder. By using a hardened steel vial and hardened steel balls, we minimized or eliminated this source of contamination. The weight of the vial and the balls after 10 successive MA experiments was the same within the 0.01 g accuracy of our balance. From this we estimate that if

impurities were introduced into the powder during MA, these amounted to less than 0.016 wt.%. We detected no iron by energy-dispersive X-ray analysis in a scanning electron microscope, which indicated that the iron content was below the 1 at.% resolution of the detector.

We used X-ray diffraction (Cu K α radiation) and differential scanning calorimetry (DSC) to study structural transformations in the as-ball-milled powder during the first oxygen anneal, as well as during the subsequent cyclic anneals. All anneals were done in flowing oxygen using cooling and heating rates of 10 °C min⁻¹ except the final cooling from 780 °C, which was done at 2 °C min⁻¹. We prepared six loose-powder samples, 100 mg each, in this manner to study the effect of 1, 2, 4, 8, 14, and 20 cyclic anneals. Following the anneals in the DSC, the powder samples had sintered into compacts that were easily removed by tilting the alumina DSC cups. There was no reaction with the alumina cups. We cyclically annealed a seventh sample, made from a pressed rod, 67 times in an oxygen-purged tube-furnace using the same heating and cooling rates.

The superconducting properties of the samples were measured by magnetic susceptibility using a Quantum Design (San Diego, CA) SQUID magnetometer.

We used scanning electron microscopy (SEM) to measure grain size and to identify phases in samples that had been studied in the DSC and had undergone susceptibility measurements. For the SEM studies, we broke the sintered samples in half. One half of each was polished using an oil-based diamond paste, and both were mounted onto aluminum holders using colloidal graphite solution. We made composition determinations on the polished samples using energy-dispersive X-ray (EDX) analysis.

The deconvolution of the EDX spectra was done with a Kevex Analyst 8000 hardware and standard-less software. Although this technique can determine the relative amounts of metallic elements in alloys such as $\text{YBa}_2\text{Cu}_3\text{O}_{7-x}$ to an accuracy no better than ± 5 at.%, this accuracy is sufficient to discern between phases such as $\text{YBa}_2\text{Cu}_3\text{O}_7$, Y_2BaCuO_5 , BaCuO_2 and CuO . The EDX detector did not allow us to detect elements with atomic number below 11.

CHAPTER IV

RESULTS

Phase Transformations During the
Synthesis of $\text{YBa}_2\text{Cu}_3\text{O}_{7-x}$

Figure 1 shows X-ray diffraction patterns of the mixed powder after 3 and 10 h of MA. After 3 h of MA the powder still has most of the Bragg peaks of the initial oxides. After 10 h of MA these peaks have disappeared and the diffraction pattern now has broad maxima and a few new Bragg peaks. The broad diffraction maxima indicate that the bulk of the powder is an amorphous oxide. Some of the new Bragg peaks belong to a cubic perovskite with lattice parameter close to the a -lattice parameter of $\text{YBa}_2\text{Cu}_3\text{O}_7$. In the figure the Bragg peaks of the cubic perovskite have been indexed in the notation of the tetragonal perovskite with $c \approx 3a$. The conclusion that the perovskite is cubic, rather than tetragonal, follows from the observation that the Bragg peaks such as (104) and (214), present in $\text{YBa}_2\text{Cu}_3\text{O}_{7-x}$, are absent in the mechanically alloyed powder. It is probable that these peaks are absent because the yttrium and barium atoms are disordered rather than arranged on the (00z) planes, alternating in the form ...Ba-Ba-Y-Ba-Ba-Y..., as required for the tetragonal form. A few Bragg peaks in curve (b) belong to phases we could not identify. During MA the powder loses oxygen; by weighing the vial and its contents before and after MA we deduce that the oxygen stoichiometry per YBa_2Cu_3 unit decreases from 8.5 in the as-mixed oxides to 7.9 ± 0.2 after 10 h of MA.

Figure 2 is a DSC trace typical of the first oxygen anneal of the as-mechanically-alloyed $\text{YBa}_2\text{Cu}_3\text{O}_x$ powder. The transformations labeled A, B1, B2 and C are

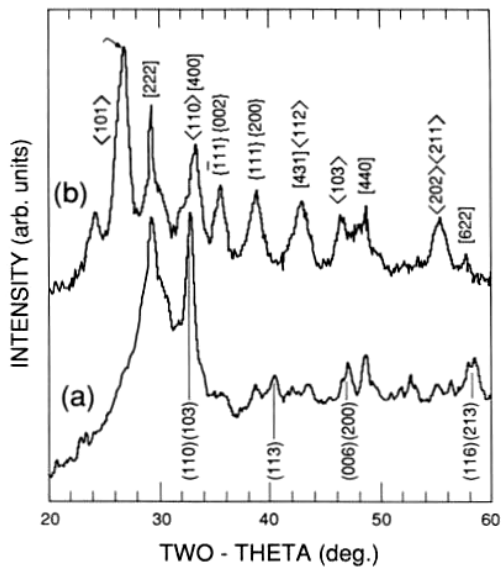


Fig. 1. X-ray diffraction patterns of mixed oxide powders after mechanical alloying for 3 h (top) and 10 h (bottom). The Bragg indices for the various compounds present are identified by bracket type: $(YBa_2Cu_3O_{7-x})$, $[Y_2O_3]$, $\langle BaO_2 \rangle$ and $\{CuO\}$.

irreversible, and the subsequent heating DSC traces show only a smooth baseline curve from 100 to 890 C. In a separate study [31] we used X-ray diffraction and thermogravimetry to identify the crystalline phases present in samples rapidly cooled from temperatures below and above peaks A, B1 and B2. These measurements enabled us to identify the transformations giving rise to these peaks. Peak A (exothermic) results from the formation of two intermediate crystalline phases: Y_2O_3 and $BaCuO_2$. Peak B1 (endothermic) is accompanied by severe oxygen loss, as evidenced by thermogravimetry [31]. This loss is immediately followed by the crystallization of the tetragonal form $YBa_2Cu_3O_{7-x}$, which gives endothermic peak B2. The small transformation labeled C only occurs during an oxygen anneal (it is absent when annealing in air) and has not yet been identified. Using the ternary $Y_2O_3 - BaO_2 - CuO$ equilibrium phase diagram proposed by Aselage and Keefer [32] we attribute endothermic peaks D and E to the

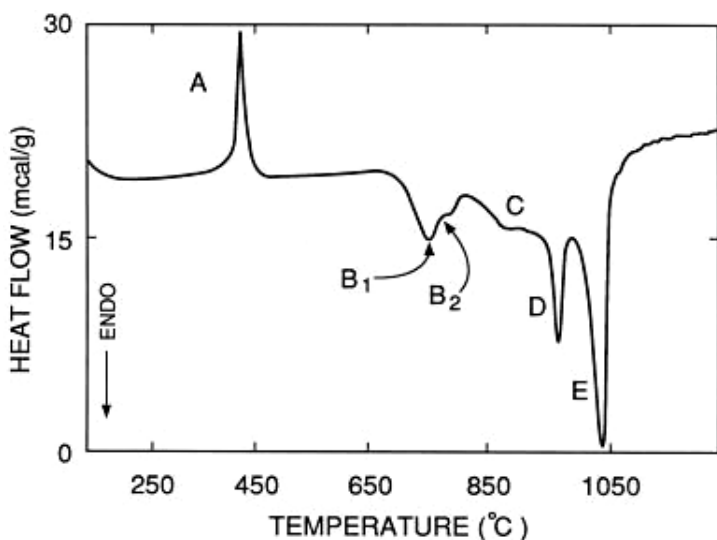
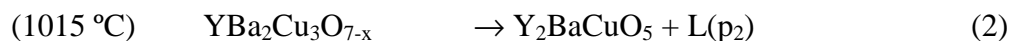
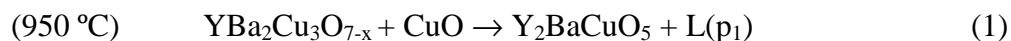


Fig. 2. DSC trace for the first oxygen anneal of the mixed alloy powders mechanically alloyed for 10 h. Sample weight = 60.80 mg.

following reactions involving the formation of melts:



The large endothermic peak E in Fig. 2 is caused by the incongruent melting of $\text{YBa}_2\text{Cu}_3\text{O}_{7-x}$ into Y_2BaCuO_5 and the peritectic liquid $\text{L}(p_2)$. Because this melt reacts with the alumina cup in the DSC, we avoided reaching this temperature in all subsequent studies.

During a DSC study involving cyclic anneals between 800 and 980 °C, we noted a continuous decrease in the enthalpy of transformation D. Figure 3 shows an overlay of DSC traces during the heating part of the first five cyclic anneals between 780 and 980 °C. The enthalpy of transformation D decreases with each cyclic anneal, whereas a new transformation at 900 °C, labeled F, appears after the sample has been cycled once. The

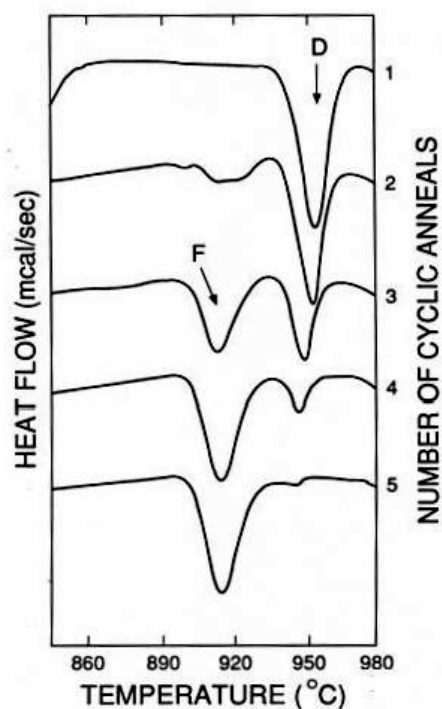


Fig. 3. DSC traces for five consecutive cyclic oxygen anneals.

area of transformation F increases with cycling, until, after 10 cycles, peak D is absent, peak F is stable, and the DSC trace is completely reversible. The enthalpies of transformations D and F are plotted as functions of the number of cyclic anneals in Fig. 4, showing the smooth, continuous nature of these changes.

To ensure that the change from peak D to peak F with cyclic anneal was not caused by a reaction between the powder and alumina in the calorimeter cups, we re-ground a sample that had been cyclically annealed four times (see curve 4 in Fig. 3) and repeated the thermal treatment in the same alumina cup. The DSC trace after re-grinding was very similar to curve 2 in Fig. 3, indicating that the transition from peak D to peak F results from reactions within the powder.

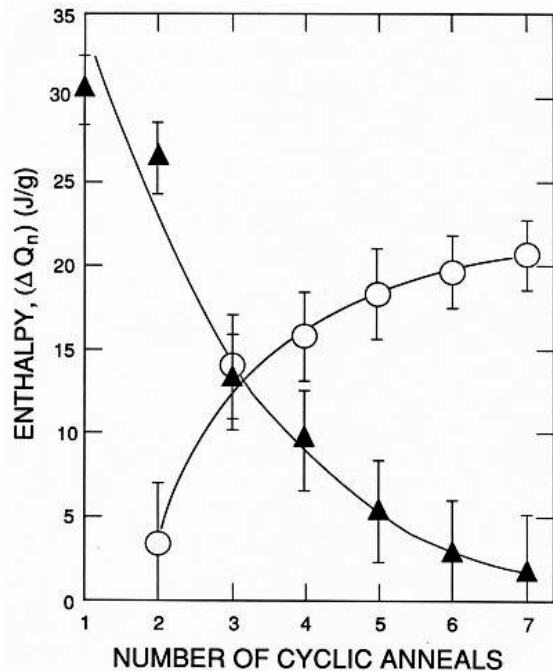
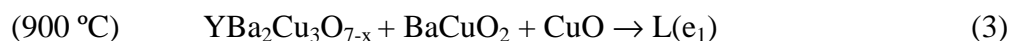


Fig. 4. Area under the DSC peaks D (filled triangles) and F (open circles) vs. number of cyclic oxygen anneals.

The ternary $Y_2O_3 - BaO_2 - CuO$ equilibrium phase diagram reported by Aselage and Kefer [32] enabled us to identify the reaction giving rise to peak F in the DSC traces as the following:



Chemistry of the Intergranular Material

We used SEM and EDX analysis to study the intergranular material in samples cyclically annealed once and 14 times. Figure 5(a) shows the backscattered electron image of a sample heated to 980 °C in flowing oxygen (i.e., above peak D in Fig. 2) and cooled to room temperature at 150 °C min⁻¹. We observed two phases. For the major light phase, EDX revealed yttrium, barium and copper in atomic ratio close to 1:2:3. The

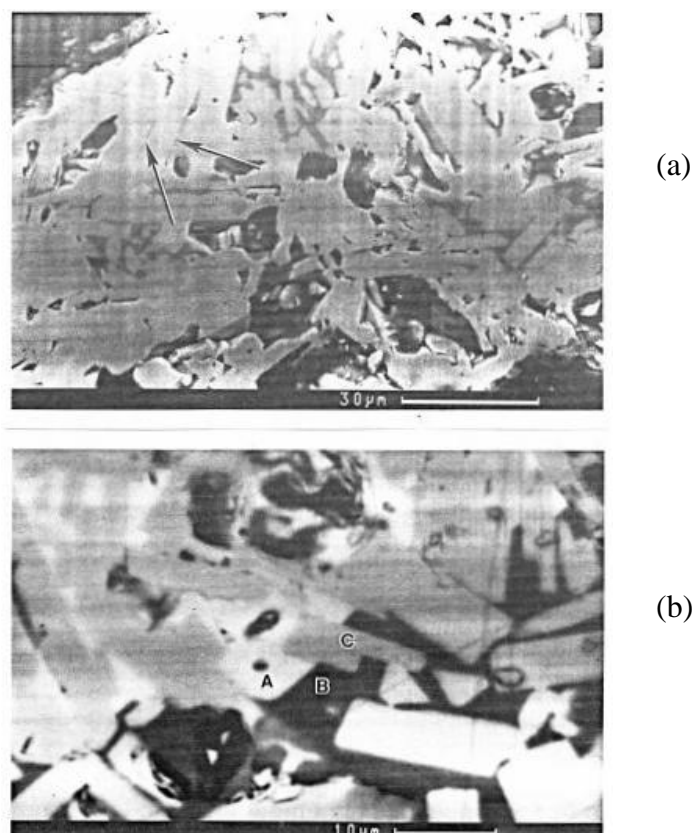


Fig. 5. Scanning electron micrographs of samples polished after 1 (a) and 14 (b) cyclic oxygen anneals. In (b), the components of the triple-point eutectic solidification are A = BaCuO_2 , B = CuO and C = $\text{YBa}_2\text{Cu}_3\text{O}_{7-x}$.

minor dark phase had only copper. The two phases present, $\text{YBa}_2\text{Cu}_3\text{O}_{7-x}$ and CuO , are those on the left hand side of eqn. (1). Notice that thin layers of CuO , indicated by the arrows, surround several $\text{YBa}_2\text{Cu}_3\text{O}_{7-x}$ crystals. We believe that, at a temperature close to 950°C but before the peritectic liquid forms for the first time, CuO is distributed uniformly throughout the sample surrounding each of the $\text{YBa}_2\text{Cu}_3\text{O}_{7-x}$ crystals. Following the reaction at 950°C , most of the CuO appears concentrated at discrete regions, which, as seen in Fig. 5(a), contain small $\text{YBa}_2\text{Cu}_3\text{O}_{7-x}$ crystallites. This agglomeration could only have resulted from the migration of the peritectic liquid $L(p1)$,

toward the more porous regions of the sample. The solidification of this liquid leads to the formation of small $\text{YBa}_2\text{Cu}_3\text{O}_{7-x}$ crystals, according to eqn. (1). We should note that Fig. 5(a) shows a region of the sample particularly rich in CuO which is not typical of the average.

The DSC trace for samples annealed 14 times shows only peak F, the 900 °C endotherm. The backscattered electron image of such a sample, shown in Fig. 5(b), reveals three phases that appear as white, light-gray, and dark-gray, labeled A, B, and C. EDX analysis reveals that A is close to a 1:1 mixture of barium and copper, phase B is yttrium, barium and copper in atomic ratio close to 1:2:3; and the dark phase C has, again, only copper. We conclude that these three phases are BaCuO_2 , $\text{YBa}_2\text{Cu}_3\text{O}_{7-x}$ and CuO, respectively. Notice in Fig. 5(b) that the three phases coexist at triple-points as required by the eutectic crystallization in eqn. (3).

Changes in the intergranular material composition are also detected by X-ray diffraction. Figure 6 shows X-ray diffraction patterns taken from samples annealed once and 20 times. The vertical scale has been enlarged. In the sample annealed once, the only Bragg peak clearly present besides those of $\text{YBa}_2\text{Cu}_3\text{O}_{7-x}$ is the (111) peak of CuO, whereas the sample cyclically annealed 20 times clearly contains $\text{YBa}_2\text{Cu}_3\text{O}_{7-x}$, CuO, Y_2BaCuO_5 , and BaCuO_2 . The presence of these phases is explained with the model discussed in Section 4.

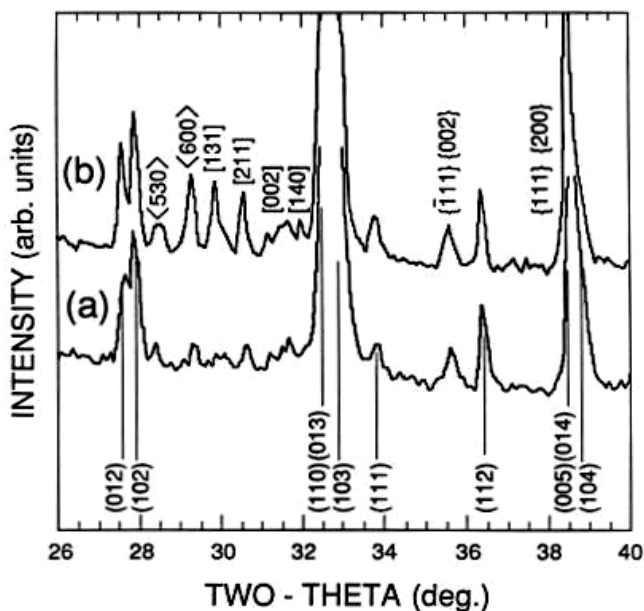
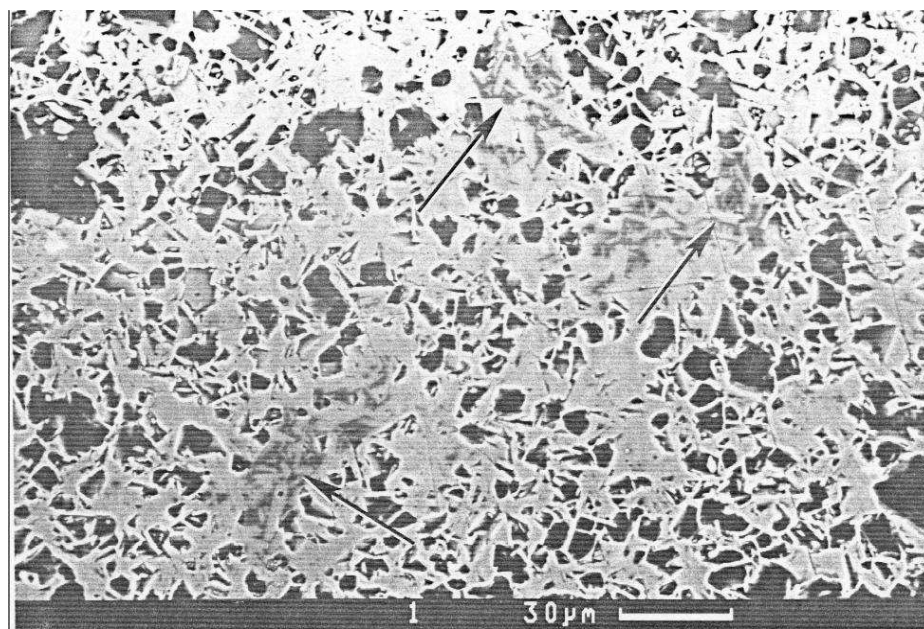


Fig. 6. X-ray diffraction patterns of $\text{YBa}_2\text{Cu}_3\text{O}_{7-x}$ cyclically annealed once (a) and 20 (b) times. The Bragg indices for the various compounds present are identified by bracket type: ($\text{YBa}_2\text{Cu}_3\text{O}_{7-x}$), [Y_2O_3], $\langle \text{BaO}_2 \rangle$ and $\{\text{CuO}\}$. Note the increased splitting between the (012) and (102) reflections after 20 cyclic oxygen anneals.

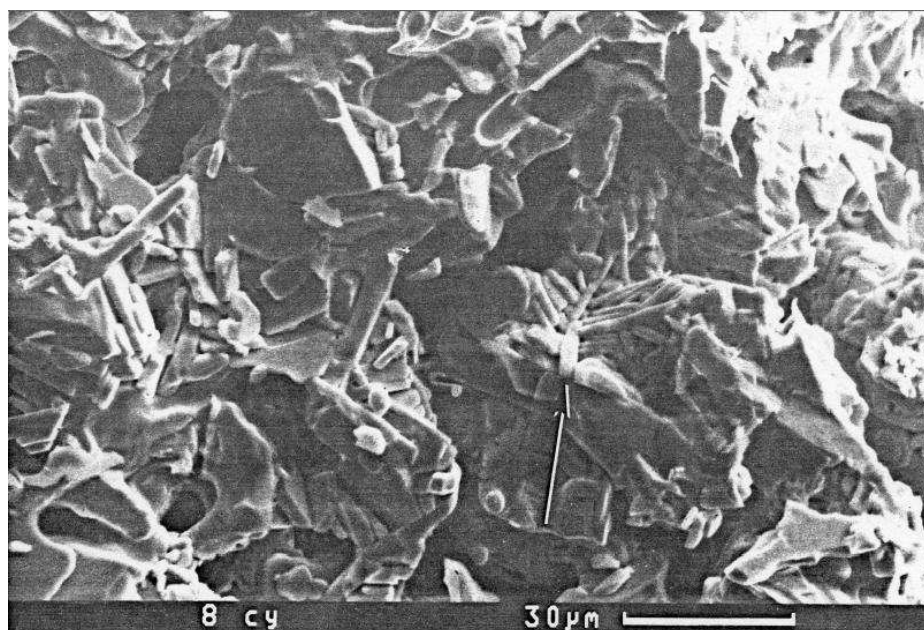
Grain Growth During Cyclic Annealing

During the cyclic anneal the average grain size increases monotonically, causing interesting changes to take place not only with regard to the grains themselves, but also in the morphology of the intergranular melts. In Figure 7 we illustrate these changes by comparing scanning electron micrographs of samples cyclically annealed 1, 8 and 67 times. The polished cross-section of a sample cyclically annealed once (Fig. 7(a)) shows the segregation and “pooling” behavior of the peritectic melt, which, upon solidifying, forms small $\text{YBa}_2\text{Cu}_3\text{O}_{7-x}$ crystals imbedded in CuO. The fracture surface of a sample cyclically annealed eight times (Fig. 7(b)) shows “feather” patterns of small $\text{YBa}_2\text{Cu}_3\text{O}_{7-x}$ crystals in the spaces between much larger crystals of $\text{YBa}_2\text{Cu}_3\text{O}_{7-x}$. This “feather”

morphology is typical of crystallization requiring phase separation during the directional freezing of liquids. The sample cyclically annealed 67 times (Fig. 7(c)) is very different;



(a)



(b)

Fig. 7. Scanning electron micrograph of samples cyclically annealed 1 (a), 8 (b), and 67 (c) times. The magnification is approximately the same for all samples. Image (a) is a backscattered electron image of a polished surface, (b) and (c) are secondary electron images of fractured surfaces.

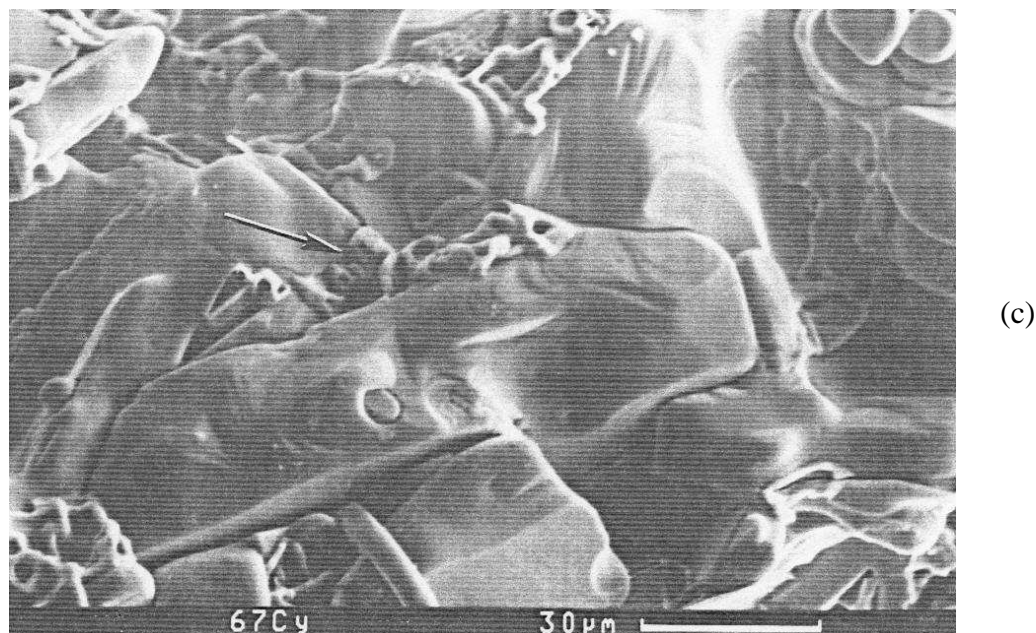


Fig. 7. (continued).

the feather patterns of small $\text{YBa}_2\text{Cu}_3\text{O}_{7-x}$ crystals are no longer in evidence. Instead, the intergranular material now appears as thin sheets of “lacy” material in spaces between large $\text{YBa}_2\text{Cu}_3\text{O}_{7-x}$ crystals. In addition, the surfaces of the large $\text{YBa}_2\text{Cu}_3\text{O}_{7-x}$ crystals show a layered morphology indicating that these crystals grew epitaxially at each thermal cycle.

Typically, $\text{YBa}_2\text{Cu}_3\text{O}_{7-x}$ crystals grow as rectangular plates with the c -axis normal to the plates, as shown in the inset of Fig. 8. This allows us to identify the c -axis by a visual inspection of SEM micrographs and to measure the dimensions of the grains. Figure 8 shows the average of crystal dimensions measured from scaled SEM photographs of fractured samples. We made no distinction between the (a) and (b) direction. Although these results only give an approximate measure of grain size, it is clear from Fig. 8 that grain size is a monotonically increasing function of the number of

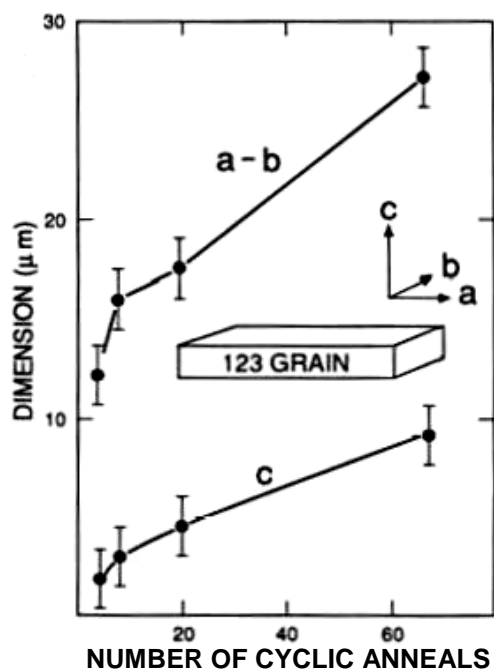


Fig. 8. Average size of the $\text{YBa}_2\text{Cu}_3\text{O}_{7-x}$ crystals vs. number of cyclic oxygen anneals.

cyclic anneals.

Besides the increase in average grain sizes, we have observed the almost complete disappearance of small ($1-10 \mu\text{m}$) $\text{YBa}_2\text{Cu}_3\text{O}_{7-x}$ grains in samples cyclically annealed more than 20 times. It became clear from examining a number of scanning electron micrographs that grain growth was accompanied by an overall narrowing of the crystal size distribution. We believe that this is caused by two phenomena:

1. Small grains of $\text{YBa}_2\text{Cu}_3\text{O}_{7-x}$ are preferentially consumed during the heating part of the cycles (formation of peritectic melt according to eqn. (1)); and
2. The surface of the large crystals is a preferred site for the nucleation of $\text{YBa}_2\text{Cu}_3\text{O}_{7-x}$ during the solidification of the peritectic melt.

Indeed, the surface of the large $\text{YBa}_2\text{Cu}_3\text{O}_{7-x}$ crystal in the center of Fig. 7(c) (sample cyclically annealed 67 times) is layered, indicating that this crystal grew in size

at each consecutive cycle by epitaxial growth from a liquid phase.

The degree of orthorhombicity, $(b-a)/a$, also increases with the number of cyclic anneals. For a sample cyclically annealed 20 times, $(b-a)/a = 1.0175 \pm 0.0005$. A sample cyclically annealed once shows only 90% of this splitting, despite an identical slow cool in flowing oxygen.

Changes in the Volume Fraction of Superconducting Phase

We determined superconducting transition temperatures (T_c) from the onset of diamagnetism in samples warmed in a d.c. magnetic field of 100 G, after zero field cooling to 7 K from room temperature. The seven samples cyclically annealed to different numbers of cycles all had T_c of 91 ± 1 K. We made magnetic susceptibility measurements at 7 K in a d.c. magnetic field of 100 G, which is lower than H_{c1} . Although the demagnetizing factor is difficult to calculate accurately, we take advantage of the fact that our samples are all of the same mass (100 mg) and external shape (that of the interior of the alumina calorimeter cup). This enables us to compare the susceptibilities and to deduce the relative fractions of superconducting phase. In Fig. 9 we have plotted susceptibility vs. number of cycles, and it is clear that the superconducting fraction increases with cyclic annealing.

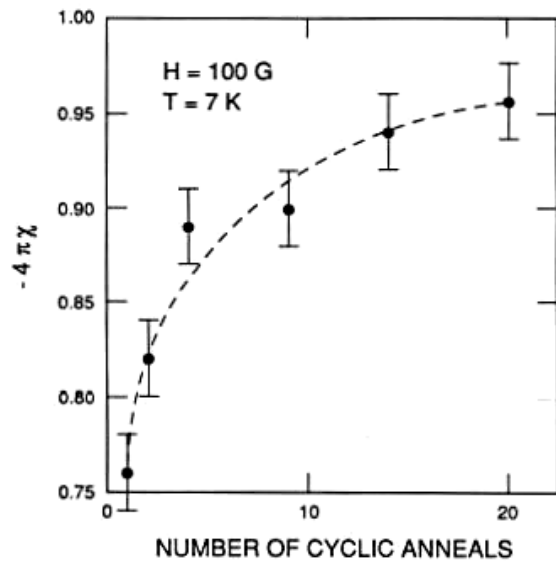


Fig. 9. Magnetic susceptibility of $\text{YBa}_2\text{Cu}_3\text{O}_{7-x}$ vs. number of cyclic oxygen anneals.

CHAPTER V

DISCUSSION

Presence of CuO at the Surface of
YBa₂Cu₃O_{7-x} Grains

According to the equilibrium phase diagram [32], single-phase YBa₂Cu₃O_{7-x} undergoes no phase transition until melting at 1015 °C. Because the reaction giving rise to peak D in the DSC trace requires the presence of CuO, the detection of this peak indicates that at 950 °C the sample has free CuO. We clearly observe CuO by SEM and X-ray diffraction in samples that were heated once to 980 °C and rapidly cooled by dropping them from the inside of a small furnace onto a copper block at room temperature. The possibility that CuO is present because of an excess of CuO in the starting mixture of oxides must be ruled out because we also observed peak D in DSC traces of samples we synthesized with deliberate copper deficiencies of 6 and 10 at.%. It might be argued that CuO forms to balance the crystallization of other copper-deficient phases such as Y₂O₃, but we have not detected any phases other than YBa₂Cu₃O_{7-x} and CuO in X-ray diffraction patterns of samples annealed once to 980 °C (Fig. 6, curve (a)). Finally, it may be argued that our intergranular material was rich in metallic impurities, as sometimes observed [33], but the EDX analysis of the dark phase in Fig. 5(a) revealed only copper (oxygen is not detected by our EDX).

We have also observed peak D in the DSC traces of YBa₂Cu₃O_x prepared by other techniques. In refs. 34 and 35 we reported the synthesis of YBa₂Cu₃O_x by the slow oxidation of YBa₂Cu₃ powder in both ¹⁸O and ¹⁶O. Peak D is clearly seen in the DSC

traces during the first heating to 980 °C in both oxygen isotopes. We have also seen peak D when analyzing in our DSC the $\text{YBa}_2\text{Cu}_3\text{O}_x$ samples prepared by other researchers [36] starting from Y_2O_3 , BaCO_3 and CuO .

The presence of CuO in nominally pure $\text{YBa}_2\text{Cu}_3\text{O}_{7-x}$ crystal at 950 °C appears to be a ubiquitous phenomenon. In fact, all DSC traces we have found in the literature [32,34,35,37-39], which span the temperature range 900 to 1000 °C show the presence of peak D. We propose tentatively that a CuO phase forms at the surface of large $\text{YBa}_2\text{Cu}_3\text{O}_x$ crystals when these are heated in air or oxygen to elevated temperatures. This phase presumably forms when copper atoms diffuse from the bulk, leaving behind constitutional vacancies and lowering the alloy's free energy. Similarly, in $\text{YBa}_2\text{Cu}_3\text{O}_x$ powder heated to high temperatures, copper would segregate at the particle surfaces. In porous aggregates, copper would segregate at the surface of interior cavities as well as exterior surfaces. From Fig. 5(a) it is apparent that grain boundaries are also effective sinks for the copper segregation.

In powder aggregates, the presence of CuO should be more noticeable in the larger particles. Suppose that at 950 °C, a fraction ε of the copper atoms in $\text{YBa}_2\text{Cu}_3\text{O}_{7-x}$ migrates to the surface of the particles. It is easy to deduce that the formation of a monolayer of CuO surrounding a spherical $\text{YBa}_2\text{Cu}_3\text{O}_{7-x}$ particle of radius r requires

$$r > 4V_y/[\varepsilon(V_c)^{2/3}] \quad (4)$$

where V_y and V_c are the volumes of the $\text{YBa}_2\text{Cu}_3\text{O}_7$ and CuO unit cells with three and four copper atoms, respectively. We have not found values for the enthalpies of vacancy formation at copper sites in bulk $\text{YBa}_2\text{Cu}_3\text{O}_x$, which would allow us to estimate ε at 950

°C. If we assume, for the sake of discussion, that $\varepsilon = 10^{-3}$, and with $V_y = 1.73 \times 10^{-28} \text{ m}^3$ and $V_c = 8.2 \times 10^{-29} \text{ m}^3$, we deduce from eqn. (4) that the formation of a monolayer of CuO requires particle sizes with $r > 3.7 \mu\text{m}$. This simple argument suggests that there is a critical particle size below which the peritectic reaction of eqn. (1) does not occur simply because there is an insufficient density of copper atoms to form a CuO phase. In this case the copper atoms that migrate to the surface of the particles heated to 950 °C would diffuse back into the bulk when they are cooled to lower temperatures. The same reversible diffusion should occur in thin films below a certain critical film thickness.

The measurement by Kuwabara and Shimooka [40] of the dependence of J_c on grain size in $\text{YBa}_2\text{Cu}_3\text{O}_x$ seem to support the model presented above. They prepared bulk samples of different average grain size d by sintering fine $\text{YBa}_2\text{Cu}_3\text{O}_x$ powder at temperatures between 920 and 950 °C for 3 to 10 h, and measured J_c in rods cut from these specimens. For $d > 2.0 \mu\text{m}$, J_c is independent of d and is close to 100 A cm^{-2} . However, $1 < d \leq 2.0 \mu\text{m}$, J_c goes through a sharp maximum, reaching values in excess of 800 A cm^{-2} . The authors attribute the increase in J_c for $1 < d \leq 1.2 \mu\text{m}$ to the increase in the density of the samples, which they also measure. They tentatively attribute the decrease in J_c for $1.2 < d \leq 2.0 \mu\text{m}$ to “residual stresses” in the samples. They also note that the decrease in J_c is accompanied by a decrease in the tensile strength of the samples. We propose as an alternative explanation for the abrupt decrease in J_c that the critical d -value for the formation of a CuO phase at the grain boundaries and at the surfaces of cavities in their $\text{YBa}_2\text{Cu}_3\text{O}_x$ samples, as defined by eqn. (4), was close to $1.2 \mu\text{m}$. Then, for $d > 1.2 \mu\text{m}$, intergranular phases would have formed by the reaction of CuO with

YBa₂Cu₃O_x as explained in ref. 32. This mechanism would also explain the observed decrease in tensile strength if the intergranular phases formed by the reaction in eqn. (1) decrease the interparticle cohesion strength. For grain sizes smaller than 1.2 μm, the density of copper atoms segregated at grain boundaries and particle surfaces is lower than that needed to form a CuO phase. On slow cooling these fine-grain samples, the copper would diffuse back into the particles, allowing the grain boundaries to remain free of second phases. Certainly, further experiments are needed to verify this model.

The foregoing discussion suggests that (a) high J_c values may be obtained in dense compacts of small grain size, as also suggested by the measurements in ref. 25; and (b) to avoid the formation of intergranular phases the sample must be sintered at temperatures below 950 °C. However, if segregated copper atoms are able to diffuse over long distances by either grain boundary or surface diffusion, then the formation of a CuO phase at high temperatures may occur even for fine grain materials and for annealing temperatures below 950 °C. Extremely slow cooling rates would then be required to allow for the copper to return to the bulk. This reverse copper migration would be facilitated by an excess of oxygen vacancies, suggesting that cooling from the sintering temperature to a temperature in the vicinity of 500 °C be made in a reduced oxygen partial pressure. Full oxygenation to reach the seven oxygens per YBa₂Cu₃ formula could be achieved by annealing in pure oxygen at 450 °C. Empirically it has been found [41] that sintering in a reduced oxygen partial pressure results in samples with large J_c .

Changes in the Intergranular Material Composition with Cyclic Annealing

We explain the progressive transition in the DSC traces from peak D to peak F on cyclic annealing with a model in which the peritectic reaction of eqn. (1) is irreversible. The main features of the model are explained with the help of Fig. 10. This figure shows, schematically, two isothermal sections of the ternary phase diagram for $Y_2O_3 - CuO - BaO$ shown in Fig. 5 of ref. 32. These sections are for the temperature $T_1 = 900\text{ }^\circ\text{C}$ (just above the ternary eutectic reaction temperature of eqn. (3)) and $T_2 = 960\text{ }^\circ\text{C}$ (just above the peritectic reaction temperature of eqn. (1)). In this figure and in the following discussion we denote a $Y_xBa_yCu_zO_p$ phase simply by (xyz) . Further details of the ternary phase diagram are shown in Fig. 5 in [32], including the position of the invariant points e_1 and p_1 inside the $(011) - (001) - (123)$ triangle.

We proposed in the previous section that when (123) is heated to temperatures close to $900\text{ }^\circ\text{C}$, the generation of constitutional vacancies at copper sites causes the formation of a small volume fraction of (001) at grain boundaries and at free surfaces. Thus, the initial alloy composition is represented by point a in Fig. 10, located along the two-phase $(123) - (001)$ tie-line. For the sake of clarity, in Fig. 10 we have exaggerated the volume fraction of (001) present and we have drawn point a farther away from point (123) than in reality. The shaded areas in Fig. 10(a) and 10(b) represent liquid. In agreement with the DSC measurements, no reaction occurs upon heating the alloy to $900\text{ }^\circ\text{C}$ for the first time because point a is on the $(123) - (001)$ tie-line. However, at $950\text{ }^\circ\text{C}$ (123) reacts with (001) forming $L(p_1)$ and (211) , according to eqn. (1). Figure 10(b)

shows that at 960 °C the sample (point *a*) is now a three-phase mixture of (123), (211) and liquid. Morphologically, (123) is the majority phase, with the (211) and liquid phases being located at the grain boundaries.

We propose that, on cooling, the (reverse) peritectic reaction of eqn. (1) is incomplete. $L(p_1)$ and (211) are not totally consumed because of a deficiency of (211) at the reaction zones. The $L(p_1)$ formed on heating migrates under capillary action and/or gravitational force, becoming separated from the (211). This separation of $L(p_1)$ and (211) can also be attributed to fractional crystallization [32], whereby (123) formed at the onset of the solidification effectively encloses the still unreacted (211) and prevents a complete reaction. The (211) left behind by the migrating peritectic liquid is no longer of consequence because no reactions occur between (211) and (123) in the temperature regime of the cyclic anneal. Removing part of the (211) phase from the reaction is equivalent to moving the alloy composition from point *a* to point *b*, as shown in Fig. 10. On cooling from 960 to 950 °C, part of the liquid solidifies into (123) and (211). On further cooling to 900 °C, part of the liquid solidifies into (123) and (001), and the remaining liquid shifts in composition toward the shaded area in Fig. 10(a). The last fraction of liquid to solidify has the eutectic composition of eqn. (3). This eutectic liquid freezes into triple-points consisting of $YBa_2Cu_3O_{7-x}$, $BaCuO_2$, and CuO , which were clearly seen in the scanning electron micrograph of Fig. 5(b). The reactions just described repeat with every thermal cycle.

At each cycle, an additional fraction of (211) becomes separated from the liquid, causing the alloy composition to stepwise move away from point (211) along the line joining points (211) and *a*. The change in the intergranular composition ceases when the

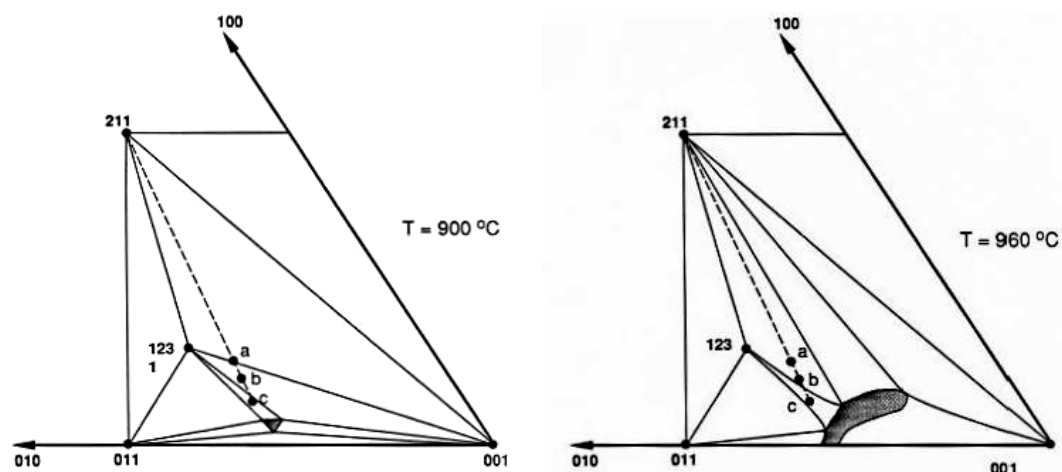


Fig. 10. Schematic isothermal sections of the ternary $Y_2O_3 - CuO - BaO$ phase diagram of Aselage and Keefer [32].

composition reaches the two-phase region $(123) - L(e_1)$, shown as point c in Fig. 10(a). Then the composition of the liquid phase remains constant for $900 < T < 960$ °C and no further changes are detected in the DSC curves during cyclic annealing. In summary, the formation of nonreacting (211) at each thermal cycle causes a decrease in the volume fraction of CuO in the intergranular material. At point c , all the CuO is tied up in the eutectic liquid and no CuO is available for the peritectic reaction that occurs on heating to 950 °C.

The model proposed here can explain quantitatively the changes in the areas under peaks D and F in the DSC traces. These areas measure the enthalpies of reaction in eqn. (1) and (3), respectively. The enthalpy of reaction D measured during the heating part of the n th cyclic anneal is proportional to the amount of CuO available at 950 °C, at the onset of the peritectic reaction of eqn. (1). As we have seen, the CuO decreases with each cycle because a fraction of the (211) does not react reversibly. If we assume that at

each cycle the CuO decreases by a fraction α , then the enthalpy of reaction D should decrease with the number of cycles, n , according to the following equation:

$$\Delta Q_{D(n)} = (1 - \alpha)^{n-1} \Delta Q_{D(1)} \quad (5)$$

Equation (5) suggests a linear plot of $\ln[\Delta Q_{D(n)}]$ vs. n . Figure 11 is such a plot, showing a linear fit for $n > 3$.

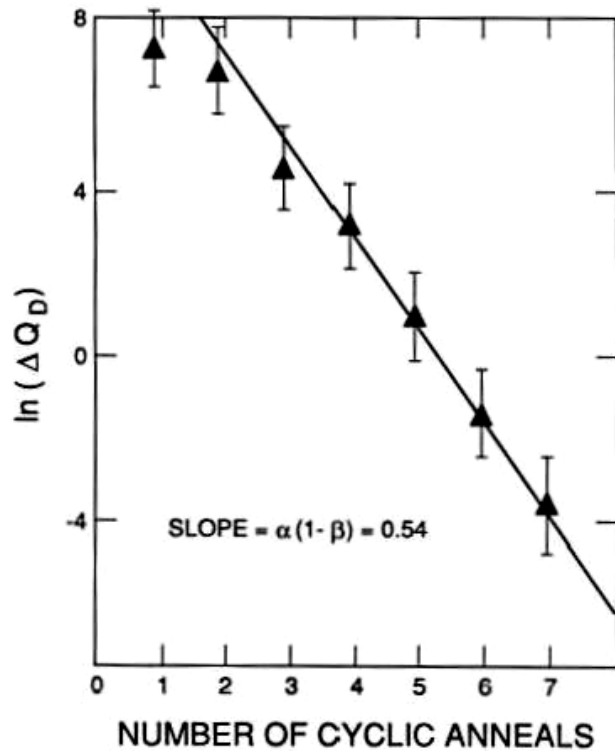


Fig. 11. Semi-log plot of the enthalpy of peak D vs. number of cyclic oxygen anneals.

CHAPTER VI

CONCLUSIONS

We propose that, when bulk $\text{YBa}_2\text{Cu}_3\text{O}_{7-x}$ is heated to near $900\text{ }^\circ\text{C}$, constitutional vacancies form at copper sites. Copper atoms segregate to grain boundaries and surfaces driven by a lowering in the crystal's free energy. The surface density of copper atoms increases with increasing grain size due to the increase in the volume-to-surface ratio. In large-grain $\text{YBa}_2\text{Cu}_3\text{O}_{7-x}$, the amount of copper is sufficient to form a CuO at grain boundaries, grain surfaces, and cavities. A CuO phase can also form in the fine-grain $\text{YBa}_2\text{Cu}_3\text{O}_{7-x}$ if the copper atoms diffuse and segregate.

Heating $\text{YBa}_2\text{Cu}_3\text{O}_{7-x}$, to $950\text{ }^\circ\text{C}$ causes the reaction of $\text{YBa}_2\text{Cu}_3\text{O}_{7-x}$ with CuO to form Y_2BaCuO_5 and liquid. On cooling, the reaction is not fully reversible because part of the liquid migrates and becomes separated from the Y_2BaCuO_5 .

The cyclic anneal of bulk $\text{YBa}_2\text{Cu}_3\text{O}_{7-x}$, between 780 and $980\text{ }^\circ\text{C}$ causes the formation of increasing amounts of Y_2BaCuO_5 at grain boundaries and voids. The volume fraction of Y_2BaCuO_5 formed this way saturates when the composition of the intergranular melt equals that of the ternary eutectic of $\text{YBa}_2\text{Cu}_3\text{O}_{7-x} + \text{BaCuO}_2 + \text{CuO}$.

REFERENCES

- 1 S. Jin, R. C. Sherwood, E. M. Gyorgy, T. H. Tieffel, R. B. van Dover, S. Nakahara, L.F. Schneemeyer, R. A. Fastnacht and M. E. Davis, *Appl. Phys. Lett.*, *54* (1989) 584.
- 2 K. Salama, V. Selvamanickam, L. Gao and K. Sun, *Appl. Phys. Lett.*, *54* (1989) 2352.
- 3 K. Watanabe, H. Yamane, H. Kurosawa, T. Hirai, N. Kobayashi, H. Iwasaki, K. Noto and Y. Muto, *Appl. Phys. Lett.*, *54* (1989) 575.
- 4 Y. D. Dai, C. Lin, W. B. Zhang, S. Q. Feng, X. Zhu, C. D. Wei, Z. X. Liu, Y. X. Sun, J. Lan, G. Z. Li, K. Wu, K. X. Chen, D. L. Yin, Z. Z. Gan, Y. F. Zhang, W. J. Zhu and B. X. Lin, *Int. J. Modern Phys. B*, *3* (1989) 77.
- 5 Y. Xu, W. Guan, K. Zeibig and C. Heiden, *Cryogen.*, *29* (1989) 281.
- 6 A. M. Hermann, Z. Z. Sheng, W. Kiehl, D. Marsh, A. El Ali, P. D. Hamburger, C. Almasan, J. Estrada and T. Datta, *J. Appl. Phys.*, *64* (1988) 632.
- 7 D. P. Hampshire, X. Cai, J. Seutjens and D. C. Larbalestier, *Supercond. Sci. Technol.*, *1* (1988) 12.
- 8 H. Kupfer, I. Apfelstedt, R. Flukiger, C. Keller, R. Meier-Hirmer, B. Runtsch, A. Turowski, U. Wiech and T. Wolf, *Cryogen.*, *29* (1989) 268.
- 9 C. P. Bean, *Phys. Rev. Lett.*, *8* (1962) 250.
- 10 C. P. Bean, *Rev. Mod. Phys.*, *36* (1964) 31.
- 11 W. A. Fietz and W. W. Webb, *Phys. Rev.*, *178* (1969) 2.
- 12 S. D. Murphy, K. Renouard, R. Crittenden and S. M. Bhagat, *Solid State Commun.*, *69* (1989) 367.
- 13 A. M. Campbell, F. J. Blunt, J. D. Johnson and P. A. Freeman, *Cryogen.*, *31* (1991) 732.
- 14 H. K. Onnes, *Comm. Phys. Lab. Univ. Leiden*, *122 and 124* (1911) 27.
- 15 W. Meissner and R. Ochsenfeld, *Naturwissenschaften*, *21* (1933) 787.
- 16 F. London and H. London, *Proc. R. Soc. London A* *149* (1935) 71.
- 17 A. Abrikosov, *Soviet Physics JETP*, *5* (1957) 1174.

- 18 V.L. Ginzburg and L.D. Landau, *Zh. Eksp. Teor. Fiz.* 20, (1950) 1064.
- 19 B. D. Josephson, *Rev. Mod. Phys.*, 46(2) (1974) 251.
- 20 J. Bardeen, L. N. Cooper and J. R. Schrieffer, *Phys. Rev.*, 108 (1957) 1175 .
- 21 J.G. Bednorz and K. A. Muller, *Z. Phys. B*, 64 (1986) 189.
- 22 M. K. Wu, J. R. Ashburn, C. J. Torng, P. H. Hor, R. L. Meng, L. Gao, Z. J. Huang, Y. Q. Wang and C. W. Chu, *Physical Review Letters*, 58 (1987) 908.
- 23 R. H. Koch, C. P. Umbach, G. L. Clark, P. Chaudhari and R. B. Laibowitz, *Appl. Phys. Lett.* 51 (1987) 200.
- 24 C. J. Humphreys, D. J. Eaglesham, N. Alford, N. McNab, M. A. Harmer and J. D. Birchall, *Inst. Phys. Conf. Ser. 93 Phys. and Mat.*, 2 (1988) 217.
- 25 R. J. Cava, B. Batlogg, R. B. van Dover, D. W. Murphy, S. Sunshine, T. Siegrist, J. P. Remeika, E. A. Reitman, S. Zuhurak and G. P. Espinoza, *Phys. Rev. Lett.*, 58 (1987) 1676.
- 26 T. R. Dinger, T. K. Worthington, W. J. Gallagher and R. L. Sandstrom, *Phys. Rev. Lett.*, 58 (1987) 2687.
- 27 P. Chaudhari, R. H. Koch, R. B. Laibowitz, T. R. McGuire and R. J. Gambino, *Phys. Rev. Lett.*, 58 (1987) 2684
- 28 B. Oh, M. Naito, S. Aronson, P. Rosenthal, R. Barton, M. R. Beasley, T. H. Geballe, R. H. Hammond and A. Kapitulnik, *Appl. Phys. Lett.*, 51 (1987) 852.
- 29 J. S. Benjamin, *Scientific American*, 234 (1976) 2.
- 30 C. Koch, O. B. Cavin, C. G. McKaney and J. O. Scarbrough, *Appl. Phys. Lett.*, 43 (1983) 1017.
- 31 A. P. Clarke and R. B. Schwarz, unpublished results, 1990.
- 32 T. Aselage and K. Keefer, *J. Mater. Res.*, 3 (1988) 1279.
- 33 L. T. Romano, P. R. Wilshaw, N. J. Long and C. R. M. Grovenor, *Supercond. Sci. Technol.*, 1 (1988) 285-90.
- 34 P. J. Yvon, R. B. Schwarz, C. B. Pierce, L. Bernardez, A. Connors and R. Meisenheimer, *Phys. Rev. B*, 39 (1989) 6690.

- 35 A. P. Clarke, P. J. Yvon, R. B. Schwarz, J. D. Thompson, R. Meisenheimer and L. Bernardez in S. H. Whang and A. D. Gupta (eds.), *High Temperature Superconducting Oxide Compounds, Processing and Related Properties*, The Materials Society, Warrendale, PA, 1989.
- 36 M. Takigawa, unpublished results, 1989.
- 37 T. H. Tieffel, S. Jin, R. C. Sherwood, M. E. Davis, G. W. Kamlitt, P. K. Gallagher, D. W. Johnson, Jr., R. A. Fastnacht and W. W. Rhodes, *Mater. Lett.*, 7 (1989) 363.
- 38 X. P. Jiang, J. S. Zhang, J. G. Huang, M. Jiang, G. W. Qiao, Z. Q. Hu and C. X. Shi, *Mater. Lett.*, 7 (1988) 250.
- 39 F. Faupel, T. Hehenkamp, K. Bente, M. Mariolakos and K. Winzer, *Physica C*, 162-4 (1989) 905.
- 40 M. Kuwabara and H. Shimooka, *Appl. Phys. Lett.*, 55 (1989) 2781-3.
- 41 U. Balachandran, R. B. Poepel, J. E. Emerson, S. A. Johnson, M. T. Lanagan, C. A. Youngdahl, Donglu Shi and K. C. Goretta, *Mater. Lett.*, 8 (1989) 454.

APPENDIX

Permissions, Waivers, and Licenses

Andrew P. Clarke
5360 Queen Ann Lane
Santa Barbara, CA 93111
(805) 705-2209
Fax: (805) 682-0250

December 7, 2007

Dr. Ricardo B. Schwarz
Los Alamos National Laboratory
Los Alamos, NM 87545

Dear Ricardo:

I am in the process of preparing my master's thesis in Physics at Utah State University. I hope to complete in the Spring of 2008.

I am requesting your permission to include the attached material as shown. I will include acknowledgments and/or appropriate citations to your work as shown and copyright and reprint rights information in a special appendix. The bibliographical citation will appear at the end of the manuscript as shown. Please advise me of any changes you require.

Please indicate your approval of this request by signing in the space provided, attaching any other form or instruction necessary to confirm permission. If you have any questions, please call me at the number above.

I hope you will be able to reply immediately.

Thank you for your cooperation,

Andrew P. Clarke

I hereby give permission to Andrew P. Clarke to reprint the following material in his thesis:

"Intergranular Phases in Cyclically Annealed YBa₂Cu₃O_{7-x}: Implications for Critical Current Densities" A.P. Clarke, R.B. Schwarz and J.D. Thompson, *Journal of the Less-Common Metals*, volume 168, pages 1-17 (February 1991). (attached.)

Signed Ricardo Schwarz Date 12/12/07.

Andrew P. Clarke
5360 Queen Ann Lane
Santa Barbara, CA 93111
(805) 705-2209
Fax: (805) 682-0250

December 7, 2007

Dr. Joseph D. Thompson
Los Alamos National Laboratory
Los Alamos, NM 87545

Dear Joe:

I am in the process of preparing my master's thesis in Physics at Utah State University. I hope to complete in the Spring of 2008.

I am requesting your permission to include the attached material as shown. I will include acknowledgments and/or appropriate citations to your work as shown and copyright and reprint rights information in a special appendix. The bibliographical citation will appear at the end of the manuscript as shown. Please advise me of any changes you require.

Please indicate your approval of this request by signing in the space provided, attaching any other form or instruction necessary to confirm permission. If you have any questions, please call me at the number above.

I hope you will be able to reply immediately.

Thank you for your cooperation,

Andrew P. Clarke

I hereby give permission to Andrew P. Clarke to reprint the following material in his thesis:

"Intergranular Phases in Cyclically Annealed YBa₂Cu₃O_{7-x}: Implications for Critical Current Densities" A.P. Clarke, R.B. Schwarz and J.D. Thompson, *Journal of the Less-Common Metals*, volume 168, pages 1-17 (February 1991). (attached.)

Signed Joe D. Thompson Date 12/7/07

**ELSEVIER LIMITED LICENSE
TERMS AND CONDITIONS**

Dec 05, 2007

This is a License Agreement between Andrew P Clarke ("You") and Elsevier Limited ("Elsevier Limited"). The license consists of your order details, the terms and conditions provided by Elsevier Limited, and the payment terms and conditions.

License Number	1842630826149
License date	Dec 05, 2007
Licensed content publisher	Elsevier Limited
Licensed content publication	Journal of the Less Common Metals
Licensed content title	Intergranular phases in cyclically annealed $\text{YBa}_2\text{Cu}_3\text{O}_{7-x}$: Implications for critical current densities
Licensed content author	Clarke A. P., Schwarz R. B. and Thompson J. D.
Licensed content date	February 1991
Volume number	168
Issue number	1
Pages	17
Type of Use	Thesis / Dissertation
Portion	Full article
Format	Print
You are an author of the Elsevier article	Yes
Are you translating?	No
Purchase order number	
Expected publication date	Jan 2008
Elsevier VAT number	GB 494 6272 12
Permissions price	0.00 USD
Value added tax 0.0%	0.00 USD
Total	0.00 USD

Terms and Conditions

INTRODUCTION

The publisher for this copyrighted material is Elsevier. By clicking "accept" in connection with completing this licensing transaction, you agree that the following terms and

conditions apply to this transaction (along with the Billing and Payment terms and conditions established by Copyright Clearance Center, Inc. ("CCC"), at the time that you opened your Rightslink account and that are available at any time at <http://myaccount.copyright.com>).

GENERAL TERMS

Elsevier hereby grants you permission to reproduce the aforementioned material subject to the terms and conditions indicated.

Acknowledgement: If any part of the material to be used (for example, figures) has appeared in our publication with credit or acknowledgement to another source, permission must also be sought from that source. If such permission is not obtained then that material may not be included in your publication/copies. Suitable acknowledgement to the source must be made, either as a footnote or in a reference list at the end of your publication, as follows:

"Reprinted from Publication title, Vol number, Author(s), Title of article, Pages No., Copyright (Year), with permission from Elsevier [OR APPLICABLE SOCIETY COPYRIGHT OWNER]." Also Lancet special credit - "Reprinted from The Lancet, Vol. number, Author(s), Title of article, Pages No., Copyright (Year), with permission from Elsevier."

Reproduction of this material is confined to the purpose and/or media for which permission is hereby given.

Altering/Modifying Material: Not Permitted. However figures and illustrations may be altered/adapted minimally to serve your work. Any other abbreviations, additions, deletions and/or any other alterations shall be made only with prior written authorization of Elsevier Ltd. (Please contact Elsevier at permissions@elsevier.com)

If the permission fee for the requested use of our material is waived in this instance, please be advised that your future requests for Elsevier materials may attract a fee.

Reservation of Rights: Publisher reserves all rights not specifically granted in the combination of (i) the license details provided by you and accepted in the course of this licensing transaction, (ii) these terms and conditions and (iii) CCC's Billing and Payment terms and conditions.

License Contingent Upon Payment: While you may exercise the rights licensed immediately upon issuance of the license at the end of the licensing process for the transaction, provided that you have disclosed complete and accurate details of your proposed use, no license is finally effective unless and until full payment is received from you (either by publisher or by CCC) as provided in CCC's Billing and Payment terms and conditions. If full payment is not received on a timely basis, then any license preliminarily granted shall be deemed automatically revoked and shall be void as if never granted. Further, in the event that you breach any of these terms and conditions or any of CCC's Billing and Payment terms and conditions, the license is automatically revoked and shall be

void as if never granted. Use of materials as described in a revoked license, as well as any use of the materials beyond the scope of an unrevoked license, may constitute copyright infringement and publisher reserves the right to take any and all action to protect its copyright in the materials.

Warranties: Publisher makes no representations or warranties with respect to the licensed material.

Indemnity: You hereby indemnify and agree to hold harmless publisher and CCC, and their respective officers, directors, employees and agents, from and against any and all claims arising out of your use of the licensed material other than as specifically authorized pursuant to this license.

No Transfer of License: This license is personal to you and may not be sublicensed, assigned, or transferred by you to any other person without publisher's written permission.

No Amendment Except in Writing: This license may not be amended except in a writing signed by both parties (or, in the case of publisher, by CCC on publisher's behalf).

Objection to Contrary Terms: Publisher hereby objects to any terms contained in any purchase order, acknowledgment, check endorsement or other writing prepared by you, which terms are inconsistent with these terms and conditions or CCC's Billing and Payment terms and conditions. These terms and conditions, together with CCC's Billing and Payment terms and conditions (which are incorporated herein), comprise the entire agreement between you and publisher (and CCC) concerning this licensing transaction. In the event of any conflict between your obligations established by these terms and conditions and those established by CCC's Billing and Payment terms and conditions, these terms and conditions shall control.

Revocation: Elsevier or Copyright Clearance Center may deny the permissions described in this License at their sole discretion, for any reason or no reason, with a full refund payable to you. Notice of such denial will be made using the contact information provided by you. Failure to receive such notice will not alter or invalidate the denial. In no event will Elsevier or Copyright Clearance Center be responsible or liable for any costs, expenses or damage incurred by you as a result of a denial of your permission request, other than a refund of the amount(s) paid by you to Elsevier and/or Copyright Clearance Center for denied permissions.

LIMITED LICENSE

The following terms and conditions apply to specific license types:

Translation: This permission is granted for non-exclusive world **English** rights only unless your license was granted for translation rights. If you licensed translation rights you may only translate this content into the languages you requested. A professional translator must perform all translations and reproduce the content word for word preserving the integrity of the article. If this license is to re-use 1 or 2 figures then permission is granted for non-exclusive world rights in all languages.

Website: The following terms and conditions apply to electronic reserve and author websites:

Electronic reserve: If licensed material is to be posted to website, the web site is to be password-protected and made available only to bona fide students registered on a relevant course if:

This license was made in connection with a course,

This permission is granted for 1 year only. You may obtain a license for future website posting,

All content posted to the web site must maintain the copyright information line on the bottom of each image,

A hyper-text must be included to the Homepage of the journal from which you are licensing at <http://www.sciencedirect.com/science/journal/xxxxx> , and

Central Storage: This license does not include permission for a scanned version of the material to be stored in a central repository such as that provided by Heron/XanEdu.

Author website with the following additional clauses: This permission is granted for 1 year only. You may obtain a license for future website posting,

All content posted to the web site must maintain the copyright information line on the bottom of each image, and

The permission granted is limited to the personal version of your paper. You are not allowed to download and post the published electronic version of your article (whether PDF or HTML, proof or final version), nor may you scan the printed edition to create an electronic version,

A hyper-text must be included to the Homepage of the journal from which you are licensing at <http://www.sciencedirect.com/science/journal/xxxxx> , and

Central Storage: This license does not include permission for a scanned version of the material to be stored in a central repository such as that provided by Heron/XanEdu.

Website (regular and for author): "A hyper-text must be included to the Homepage of the journal from which you are licensing at

<http://www.sciencedirect.com/science/journal/xxxxx>."

Thesis/Dissertation: If your license is for use in a thesis/dissertation your thesis may be submitted to your institution in either print or electronic form. Should your thesis be published commercially, please reapply for permission. These requirements include permission for the Library and Archives of Canada to supply single copies, on demand, of the complete thesis and include permission for UMI to supply single copies, on demand, of the complete thesis. Should your thesis be published commercially, please reapply for permission.

Other conditions: None
